

The effects of a dynamic lattice on methane self-diffusivity calculations in $\text{AlPO}_4\text{-5}$

Kendall T. Thomson,^{a)} Alon V. McCormick, and H. Ted Davis
Department of Chemical Engineering and Materials Science, University of Minnesota, Minneapolis, Minnesota 55455

(Received 18 August 1999; accepted 11 November 1999)

Canonical ensemble molecular dynamics simulations were conducted for methane diffusion in $\text{AlPO}_4\text{-5}$ in order to assess the role of the lattice motion on adsorbate diffusivity in straight pore zeolites. Both a static lattice model and a full dynamic lattice model were used at a loading of 1.5 methane/unit cell at 295 K. Although recent simulation work has asserted that there should be a difference, we show that there is little difference in the observed methane diffusivity ($1.26 \times 10^{-7} \text{ m}^2/\text{s}$) and passing frequency (0.305) when a static lattice approximation is used over a full dynamic lattice ($1.33 \times 10^{-7} \text{ m}^2/\text{s}$ and 0.328). Furthermore, we introduce a methodology for handling lattice motion in molecular simulations by utilizing the normal vibrational modes in a harmonic crystal approximation. © 2000 American Institute of Physics. [S0021-9606(00)70406-5]

I. INTRODUCTION

The study of diffusion in confined geometries has seen a considerable effort lately.¹⁻¹⁸ A common objective is to better understand catalysis in commercial zeolite systems. For example, if the time scale for diffusion is remarkably slower than the specific reaction rate of a given catalyst, the overall conversion is poor. Likewise, adverse reactions or accelerated conversion rates can dominate, causing unwanted selectivities or excess coking in cracking catalysts.¹⁹ There is consequently a strong motivation for predicting diffusivities in such systems.

Zeolites are the materials one usually has in mind when considering confined geometries. Besides their commercial relevance as catalysts, adsorbents, and molecular sieves, diverse zeolite structures offer a large spectrum of environments for studies of diffusion. The rich selection of pore and cavity topologies offered by zeolites—including diffusion pathways of different dimensionality—has produced diffusion phenomena that is lacking in the conventional, unconstrained geometries. Consequently, zeolites offer an experimental test of theoretical models that explore the particulars of molecular confinement.

A classic example of such phenomena is the problem of single-file versus unidirectional diffusion in one-dimensional pores. The zeolite $\text{AlPO}_4\text{-5}$ can be structurally characterized as a one-dimensional pore system (Fig. 1). Pores are arranged in a hexagonal pattern and bounded by 12-fold oxygen rings. The constricting nominal diameter is 7.3 Å (10.0 Å from oxygen centers); however, the wall diameter oscillates along the pore direction to up to 7.9 Å.

The nominal diameter of $\text{AlPO}_4\text{-5}$ pores leads one to believe that methane molecules, with a Lennard-Jones effective diameter of 3.88 Å, would be unable to pass one another while confined in the pores (defined as single-file diffusion). However, pulsed-field gradient (PFG) nuclear magnetic reso-

nance (NMR) experiments by Gupta and Nivarthi,¹⁶ as well as quasielastic neutron scattering experiments by Jobic and others,¹⁷ show that methane does exhibit unidirectional diffusion (defined as unconstrained, one-dimensional diffusion where passing is allowed). Similarly, Keffer¹⁸ has offered evidence from canonical molecular dynamics simulations that unidirectional diffusion of methane occurs in $\text{AlPO}_4\text{-5}$.

On the other hand, PFG-NMR experiments by Kärger and others^{13,20} show unexpectedly low diffusivities for methane, and single-file diffusion was observed for CF_4 in $\text{AlPO}_4\text{-5}$. These contradictory findings are as yet unexplained, and it seems reasonable that molecular dynamics simulations could prove beneficial in resolving the issue. However, it is important to be sure that a given simulation model is accurate enough to draw proper conclusions. For example, the molecular dynamics simulation of Keffer incorporated a spherical Lennard-Jones interaction model for methane. As a result, the structural detail of the methane molecule was neglected. Furthermore, a *static lattice approximation* was made whereby the lattice atoms were held fixed in their crystallographical positions throughout the simulation.

There is conflicting evidence in the literature as to the validity of static lattice model. Keffer²¹ showed that the static lattice approximation produced diffusivities nearly identical to that obtained from a fully dynamical lattice for xenon in $\text{AlPO}_4\text{-5}$. Similarly, Smirnov¹⁰ concluded that methane characteristics are not significantly affected by framework flexibility. However, several authors have seen moderate to drastic differences in diffusivity when making the same comparison in different systems.^{2,4-6,8}

In this paper, we tested the validity of the static lattice approximation by conducting canonical molecular dynamics simulations of methane in an $\text{AlPO}_4\text{-5}$ pore. The methane molecules were treated as rigid units consisting of a single carbon atom tetrahedrally bonded to four hydrogen atoms. We used pairwise additive potentials to represent methane—

^{a)}Electronic mail: thomson@unity.ncsu.edu

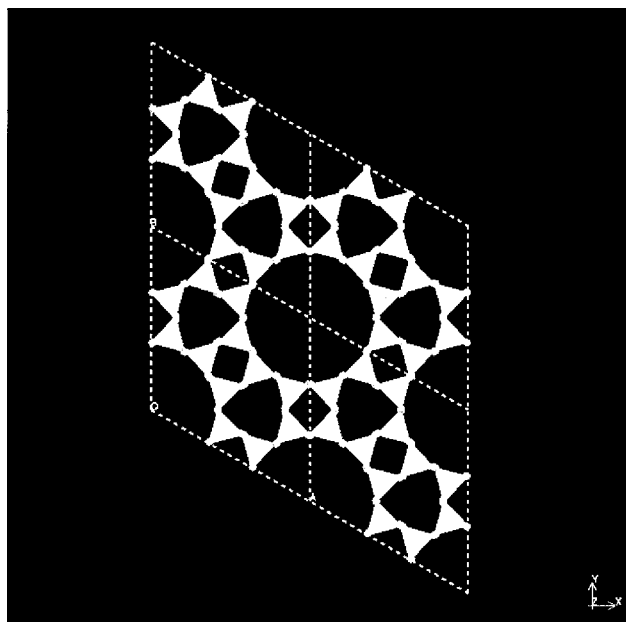


FIG. 1. The crystallographic structure of $\text{AlPO}_4\text{-5}$ along the hexagonal unit cell c axis.

methane and methane–oxygen interactions. Simulations were conducted using both a static lattice (with fixed lattice molecules) and a dynamic lattice. In the latter, the collective motion of the zeolite lattice was handled through a full dynamical treatment of the normal modes of $\text{AlPO}_4\text{-5}$ (limited to a finite periodicity). The details of the method are provided below.

II. SINGLE-FILE VERSUS UNIDIRECTIONAL DIFFUSION

It is well-known that diffusive processes can be expressed stochastically by introducing the diffusion propagator $P(\mathbf{r}-\mathbf{r}_0;t)$, which describes the probability of a particle being found at position \mathbf{r} at time t , given that it was located at \mathbf{r}_0 at time $t=0$. For unidirectional ordinary diffusion, the propagator takes the form

$$P(x-x_0;t) = \frac{1}{\sqrt{4\pi Dt}} \exp\left(-\frac{(x-x_0)^2}{4Dt}\right), \quad (1)$$

where D is the traditional diffusivity of the diffusion equation. A consequence of the above equation is that the long time mean-square displacement of a particle is given by Einstein's equation²²

$$\lim_{t \rightarrow \infty} \langle (x-x_0)^2 \rangle = 2Dt. \quad (2)$$

The above expression holds for unidirectional diffusion in pores where molecules are allowed to pass one another. However, for single-file diffusion, Einstein's equation does not hold. Rather, it can be shown²⁰ the long time mean-square displacement is proportional to the square root of time

$$\lim_{t \rightarrow \infty} \langle (x-x_0)^2 \rangle \propto \sqrt{t}. \quad (3)$$

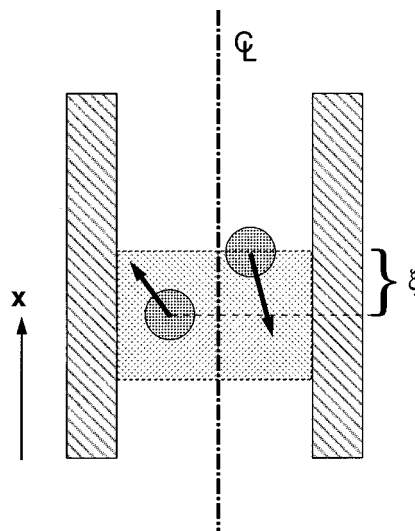


FIG. 2. A passing event for defining the passing frequency.

This qualitative difference in diffusion modes can be observed in either experiment or simulation, provided the correct time scale is observed. That is to say, a large enough sample time must be realized in order to approximate the infinite time limits in the above equations.

One way to characterize diffusion is in the passing frequency η , which we define as the fraction of passing attempts that succeed. In a one-dimensional pore—with diameter such that confinement is evident—a passing attempt is “counted” when any two centers of mass of the appropriate molecules pass within a certain tolerance ξ (see Fig. 2). Thus, in a given simulation we would measure the distance along the pore direction of every molecule and note when the difference between any two molecules is less than this tolerance, i.e.,

$$|x_i - x_j| < \xi.$$

When the molecules separate again (i.e., when $|x_i - x_j|$ again exceeds ξ) we note whether their positions have switched (i.e., the sign of $x_i - x_j$ has changed) to determine if the attempt was successful.

Of course, the passing frequency of a given simulation will depend on the tolerance ξ used. We chose the Lennard-Jones diameter of methane for this work. Although this seems arbitrary, it is only important that we are consistent in our application, especially when comparisons in techniques are being made.

The parameter ξ serves as a measure of the degree of single-file diffusion. As the effective diameters of the molecules approach some critical value, η will approach zero. In such cases where passing events are rare, it is possible that molecules may not be observed to pass each other within the chosen time scale of a given simulation or experiment. Single-file behavior would then be observed and Eq. (2) would hold. However, if the time scale were made large enough such that enough passing attempts were sampled, unidirectional diffusion would become evident. It is there-

TABLE I. Potential parameters for Al, P, and O used during structural relaxation of the AlPO₄-5 framework. Taken from Ref. 21.

	a_{ij} (eV)	b_{ij} (Å ⁻¹)	c_{ij} (eV-Å ⁶)	q_i (a.u.)
Al-O	16 008.5345	4.796 67	130.5659	...
P-O	9 034.2080	5.190 98	19.8793	...
O-O	1 388.7730	2.760 00	175.0	...
Al	1.4
P	3.4
O	-1.2

fore important to insure the time scale of a given experiment/simulation is large enough such that the observed passing frequency η_{obs} approaches the true value.

III. SIMULATION METHODS

A. Structural minimization

The lattice parameters and atomic equilibrium positions of AlPO₄-5 were obtained from the minimum energy configuration through a damped, variable cell molecular dynamics simulation. The starting configuration was taken from experimental x-ray diffraction data.²³ Simultaneous relaxation of the unit cell and atomic positions was then conducted with damping until the total enthalpy converged to within 0.001 kJ/(mole TO₂), and atomic positions to within 0.005% of the unit cell dimensions.

The interaction energies were taken from Kramer *et al.*²⁴ and consisted of a van Beest-type repulsion with r -6 dispersion and a Coulombic term. The form of the interaction potential was

$$U_{ij}(r) = a_{ij} \exp(-b_{ij}r) - \frac{c_{ij}}{r^6} + \frac{q_i q_j}{r},$$

where i and j correspond to either Al, P, or O atoms. Only Al-O, P-O, and O-O interactions were included for the van Beest potentials; however, all combinations are included in the Coulomb interaction energy. Values for the potential parameters are given in Table I.

The resulting structural parameters are included in Table II. We calculated a total potential energy of -5691.2 kJ/(mole TO₂) which is within 0.02% of de Man *et al.*,²⁵ who reported a value of -5690.05 kJ/mole using the same potentials. The minimum and maximum pore diameters (measured from oxygen centers) were 10.56 and 11.58 Å,

TABLE II. Atomic potential parameters for C-C, C-H, and H-H interactions used for methane-methane and methane-lattice interactions. Taken from Refs. 24 and 25.

	a_{ij} (eV)	b_{ij} (Å ⁻¹)	c_{ij} (eV-Å ⁶)	ϵ (eV)	σ (Å)
C-C	2684.1	1.0081	21.898
C-H	476.99	1.0277	5.5504
H-H	114.00	1.0473	1.4005
O-C	0.003 444 2	3.6713
O-H	0.002 229 5	3.1782

TABLE III. Structural parameters and internal coordinates of AlPO₄-5.

	This work	Experiment (Ref. 23)
a (Å)	14.174	13.736
c (Å)	8.675	8.484
Al	(0.4538, 0.3334, 0.4531)	
P	(0.4539, 0.3312, 0.0789)	
O(1)	(0.4553, 0.3341, 0.2526)	(0.4550, 0.3312, 0.2500)
O(2)	(0.5647, 0.4183, 0.0208)	(0.5684, 0.4126, 0.0140)
O(3)	(0.3727, 0.3621, 0.0199)	(0.3670, 0.3584, 0.0260)
O(4)	(0.4302, 0.2216, 0.0221)	(0.4210, 0.2137, 0.0280)

respectively. These values are noticeably larger than the experimental values²³ (9.99 and 11.17 Å); thus, an artificially larger pore resulted.

B. Methane potentials

The resulting atomic positions were then used for the static lattice molecular dynamics simulations and as the equilibrium positions in the dynamic lattice simulation. In all cases, a single pore of AlPO₄-5 was used and a pore length of 2 unit cells along the pore direction was chosen. Interactions of the pore with adsorbate molecules only included the O-Me interactions (oxygen-methane), as is common practice.²¹ Methane was assumed to be a rigid molecule with fixed C-H bond lengths of 1.094 Å. The Me-Me interactions were handled by pairwise additive potentials for C-C, C-H, and H-H as given by Murad, Evans, and Gubbins.²⁶ A van Beest interaction potential with r -6 dispersion was assumed for each atom combination and is given below

$$U_{ij}(r) = a_{ij} \exp(-b_{ij}r) - \frac{c_{ij}}{r^6}.$$

The force field parameters (Table III) were previously shown to accurately represent the thermodynamic properties of methane at nominal conditions and produced adequate diffusivities in bulk.²⁶

The framework O-Me interactions were handled with pairwise additive Lennard-Jones-like 12-6 potentials for O-C and O-H given by

$$U_{ij}(r) = \epsilon_{ij} \left(\left(\frac{\sigma_{ij}}{r} \right)^{12} - 2 \left(\frac{\sigma_{ij}}{r} \right)^6 \right).$$

The parameters were taken from the universal force field potentials (UFF) of Rappe and others²⁷ and are given in Table III. A cutoff radius of 15 Å was used for all potential terms and we used the shifted-force method^{22,28-31} to assure proper energy convergence.

C. Dynamic lattice model

In the static lattice model, all zeolite atoms were held fixed at their calculated minimum energy equilibrium positions (obtained with an empty pore). For the dynamic lattice model, we included the framework oxygen degrees of freedom in the dynamics. We handled the lattice-lattice interactions by solving for the vibrational modes of a 2 × 2 × 2 supercell of AlPO₄-5. We then applied the harmonic crystal approximation, whereby each mode acted as a free oscillator.

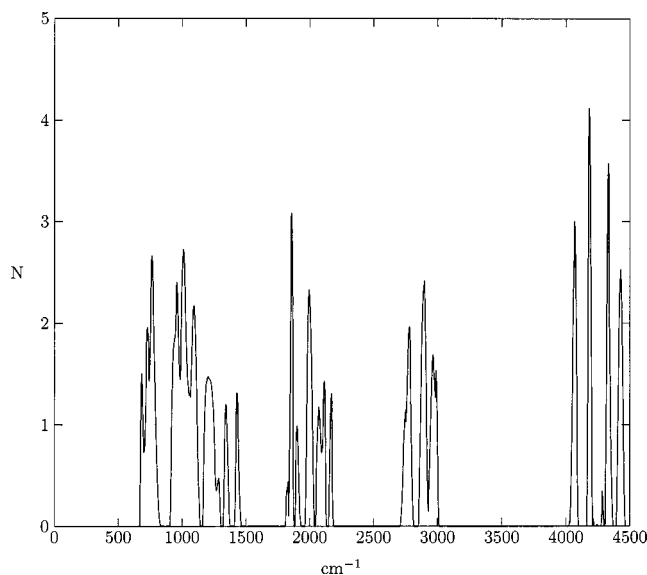


FIG. 3. Eigenspectrum for the normal modes of a $2 \times 2 \times 2$ supercell of $\text{AlPO}_4\text{-5}$. The density distribution is given in arbitrary units.

The vibrational modes were calculated from the equilibrium positions of the $\text{AlPO}_4\text{-5}$ lattice obtained during the structural relaxation (Fig. 3). For a supercell containing N atoms, we can define the equilibrium positions by the $3N$ dimensional vector $\bar{\mathbf{r}}$, where

$$\bar{\mathbf{r}} = \begin{pmatrix} \bar{x}_1 \\ \bar{y}_1 \\ \bar{z}_1 \\ \bar{x}_2 \\ \vdots \\ \bar{y}_N \\ \bar{z}_N \end{pmatrix},$$

and \bar{x}_n refers to the x component of the equilibrium position of the n th ion. The displacement from equilibrium can then be represented by the vector \mathbf{u} defined by $u_i \equiv \sqrt{m_i}(r_i - \bar{r}_i)$, where m_i refers to the atomic mass of the ion represented by the i th position. The decoupled Lagrangian for the dynamic lattice model can then be given by

$$\mathcal{L}_{\text{dynamic}} = \mathcal{L}_{\text{static}} + \frac{1}{2} \dot{\mathbf{w}}^T \dot{\mathbf{w}} - \frac{1}{2} \mathbf{w}^T \Lambda \mathbf{w} - U_0.$$

Λ is diagonal and contains the normal mode frequencies of the supercell. The vector \mathbf{w} represents the *mode displacements* and is related to the true atomic displacements through the linear transformation

$$\mathbf{w} \equiv \mathbf{X}^T \mathbf{u},$$

where \mathbf{X} results from the diagonalization of the second-order terms in the lattice interaction energy.

The equations of motion for the modes are easily derived by noting that the ion positions \mathbf{r} are related to the mode displacements \mathbf{w} by

$$r_i = \bar{r}_i + \frac{1}{\sqrt{m_i}} \sum_{j=1}^{3N} X_{ij} w_j. \quad (4)$$

Defining the *external force*—i.e., the force on a lattice atom due to the collective interaction with the adsorbates—on ion-component i as

$$f_i = - \frac{\partial U}{\partial r_i},$$

the equations of motion for the mode displacements become

$$\ddot{w}_i = -\lambda_i w_i + \frac{1}{\sqrt{m_i}} \sum_{j=1}^{3N} X_{ji} f_j. \quad (5)$$

The above equations of motion have several advantages versus conventional treatments of lattice motions. First, by applying the harmonic crystal approximation, the time-consuming computations of the the Ewald energy due to the Coulombic interactions are eliminated. Second, the calculation of the forces in the mode equations of motion are greatly simplified. We no longer have to calculate the $3N(3N-1)$ interaction terms for the lattice degrees of freedom. Rather, we store the matrix \mathbf{X} , compute the relevant forces (f_i) at each time step, then apply the linear transformation in Eq. (5) for each mode. Furthermore, matrix-vector multiplication is an easily parallelizable operation, adding even greater performance on parallel processing platforms.

One final note—we did not have to store the complete matrix \mathbf{X} . Since we only counted interactions (and thus forces) on the framework oxygen atoms, we needed to store only the components of \mathbf{X} needed to transform r_i and f_i in Eqs. (4) and (5). It is interesting that even though the mode dynamics intrinsically determines the trajectories of the metal ions (Al and P), they are never explicitly calculated. This is because they are irrelevant to our calculation—so long as no external forces are acting on them (i.e., from methane–lattice interactions).

IV. RESULTS

A. Calculation details

We conducted both static lattice and dynamic lattice canonical molecular dynamics on a single $\text{AlPO}_4\text{-5}$ pore with a loading of 1.5 methane per unit cell at 295 K. Three methane molecules were randomly placed in our simulation pore (composed of two unit cells along the pore direction) and 50 000 canonical Monte Carlo steps were conducted in order to eliminate unusually high initial forces due to chance overlap. Both methane position and orientation as well as normal mode displacements were allowed in the Monte Carlo steps in order to initialize the normal vibrational degrees of freedom. Initial velocities and angular velocities were assigned by randomly sampling from a Boltzmann distribution. Total linear momentum was then set equal to zero and all velocities were rescaled to give temperatures equal to 295 K (note that kinetic energy was assumed to be equally partitioned among linear and angular degrees of freedom for methane, and normal modes).

An induction period of 5 ns was conducted for each run in order to equilibrate the system. This was followed by a production period of 120 ps in which data were sampled every 50 time steps. A relatively small time step was needed

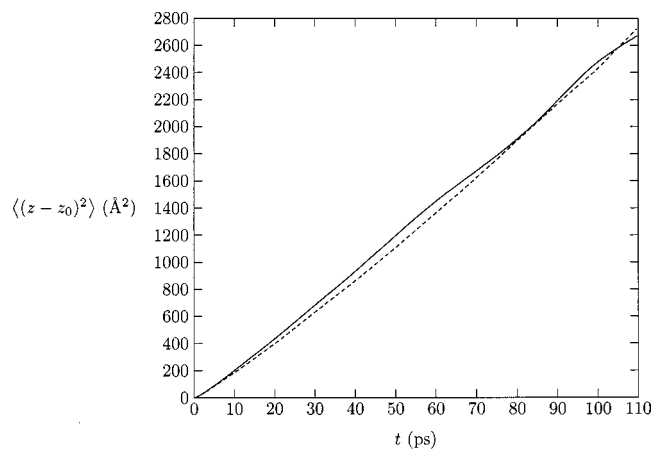


FIG. 4. Mean squared displacement of methane in $\text{AlPO}_4\text{-5}$ for the static lattice model (solid line) and the dynamic lattice model (dashed line).

(0.25×10^{-15} s) due to the methane rotational motion and the framework vibrational motion. The temperature was held at 295 K by velocity rescaling every 15 time steps. Rescaling was done separately on the linear methane, angular methane, and normal mode degrees of freedom. Constant energy runs were conducted before beginning the canonical runs and no energy drift was observed. A total of 30 runs was conducted for both the static and dynamic lattice calculations, resulting in a total of 90 methane molecules for statistical averaging. The square displacements for each molecule were recorded and the mean square displacement was determined using multiple time origins³² plus averaging over all molecules. Figure 4 shows the mean square displacement for both static and dynamic lattice calculations. The passing frequencies were calculated as described in Sec. 6.3 and averaged over all 30 runs for both lattice models (see Table IV).

B. Methane diffusivity

The mean square displacement was found to be linear with time for both the static and dynamic lattice models, suggesting that methane exhibited unidirectional diffusion for both cases. The diffusivities were determined by linear regression of the mean square displacement—Eq. (2)—using points between 40 and 110 ps. We report a diffusivity of $1.26 \times 10^{-7} \text{ m}^2/\text{s}$ for the static lattice model and $1.33 \times 10^{-7} \text{ m}^2/\text{s}$ for the dynamic lattice model. The observed passing frequencies were found to be 0.305 and 0.328 for the static and dynamic lattice models, respectively. Clearly, there were successful passing events in both models, and unidirectional diffusion for methane is confirmed. Likewise, the passing frequencies reflect the observed diffusivities for

both models. That is to say, the higher passing frequency observed for the dynamic lattice model correlates with the higher observed diffusivity.

The similarity between the observed diffusivities for the two lattice models suggests that the dynamic effect of the lattice on methane diffusion is small. One could speculate that a nonstatic lattice would be able to expand during a passing attempt, accommodating the increased local stress from the passing methanes. This would facilitate passing and result in a higher observed diffusivity. However, in this study methane molecules are not substantially inhibited from passing by the pore walls—as demonstrated by the relatively high passing frequencies we observed. We suspect that such lattice modifications would only be important when passing is severely hindered (i.e., when $\eta \rightarrow 0$).

Our results differ from a previous calculation for methane diffusion in silicalite¹⁰ where the diffusivity in a dynamic lattice was found to be considerably higher than in a static lattice. However, calculations of methane self-diffusivities in a Type A zeolite lattice¹¹ concluded that there was no significant difference between a static and fully dynamic lattice over a wide temperature range. In silicalite, the diameter of the pore constrictions is significantly less than in $\text{AlPO}_4\text{-5}$ (5.3 versus 7.4 Å) and in Linde Type A. Even though unidirectional diffusion was observed in silicalite, the effects of lattice modifications due to the dynamic lattice could have accounted for such a drastic difference in observed diffusivities. Furthermore, it is unclear to what degree thermal oscillations of the framework oxygen positions have on methane diffusivity. It seems reasonable that thermal fluctuations in the framework would on average have no net effect on diffusivity. If this were the case, we would expect the effect of the lattice motions to be temperature independent. One possible way to test this would be to run simulations of both lattice models at different temperatures.

Our observed diffusivities were around 2 orders of magnitude higher than the PFG-NMR experimental value of $1.15 \times 10^{-9} \text{ m}^2/\text{s}$ from Gupta *et al.*¹⁶ at 295 K and 1.5 methane/pore. Our diffusivities were also around twice that of Keffer's simulated value of $4.8 \times 10^{-8} \text{ m}^2/\text{s}$ at 295 K. The higher diffusivities in our and Keffer's calculations can be partially attributed to the larger pore size obtained during structural minimization (Keffer used identical potentials to represent lattice–lattice interactions). The actual x-ray diffraction (XRD) determined oxygen positions in $\text{AlPO}_4\text{-5}$ result in a more constricted pore which should necessarily result in lower diffusivities. It seems, however, that by adding structure to the methane molecule we have widened the gap between simulation and experiment (by a factor of 2 compared to a spherical Lennard-Jones representation of methane). Most likely this is not due to the five-point methane model by Murad, Evans, and Gubbins,²⁶ but rather due to our methane–framework interaction potentials. A previous calculation by June, Bell, and Theodorou³³ using a similar five-point methane model produced essentially qualitative agreements with experimental diffusivities. Future work should therefore consider replacing the UFF interaction potentials for methane–oxygen with a more sophisticated potential. Models suggested by Kiselev³⁴ and by Pellenq and

TABLE IV. Calculated diffusivities and passing frequencies of methane in $\text{AlPO}_4\text{-5}$.

	Static lattice	Dynamic lattice
$D \text{ (m}^2/\text{s)}$	1.26×10^{-7}	1.33×10^{-7}
η	0.305	0.328

Nicholson^{35,36} have yielded accurate adsorption properties for methane in $\text{AlPO}_4\text{-5}$ (Ref. 37) and are thus good candidates.

V. CONCLUSIONS

We have shown that the static lattice model yields similar diffusivities to those obtained with a fully dynamic lattice in canonical molecular dynamics simulations in $\text{AlPO}_4\text{-5}$. The difference in diffusivities was found to be less than a 6% deviation. It is apparent that the flexibility of the dynamic lattice does not significantly enhance diffusion when passing events are frequent, although as the passing frequency approaches zero, it is possible that a flexible lattice may enhance diffusion by reducing the energy barrier for passing events. What effect the thermal vibrations would have on such a scenario is uncertain and future calculations at varying temperatures are planned.

We have also shown that methane exhibits unidirectional diffusion in $\text{AlPO}_4\text{-5}$. This agrees with experimental results, although the disagreement between measured and simulated diffusivities casts a shadow on the quality of the interaction potentials. We have also shown that the passing frequency η appears to be a good measure of the degree of unidirectional versus single-file diffusion modes in confined geometries.

¹L. Leherter, D. P. Vercauteren, E. G. Derouane, G. C. Lie, E. Clementi, and J.-M. Andre, in *Zeolites: Facts, Figures, Future; Proceedings of the 8th International Zeolite Conference, Amsterdam, 1989*, edited by P. A. Jacobs and R. A. van Santen (Elsevier, Amsterdam, 1989), p. 773.

²P. Demontis, E. S. Fois, G. B. Suffritti, and S. Quartieri, *J. Phys. Chem.* **94**, 4329 (1990).

³A. K. Nowak, C. J. J. den Ouden, S. D. Pickett, B. Smith, A. K. Cheetham, M. F. M. Post, and J. M. Thomas, *J. Phys. Chem.* **95**, 848 (1991).

⁴C. R. A. Catlow, C. M. Freeman, B. Vessal, S. M. Tomlinson, and M. Leslie, *J. Chem. Soc., Faraday Trans.* **87**, 1947 (1991).

⁵P. Demontis, G. B. Suffritti, E. S. Fois, and S. Quartieri, *J. Phys. Chem.* **96**, 1482 (1992).

⁶P. Demontis, G. B. Suffritti, and P. Mura, *Chem. Phys. Lett.* **191**, 553 (1992).

⁷P. Demontis and G. B. Suffritti, *Chem. Phys. Lett.* **223**, 355 (1994).

⁸S. Bandyopadhyay and S. Yashonath, *Chem. Phys. Lett.* **223**, 363 (1994).

⁹S. Yashonath and S. Bandyopadhyay, *Chem. Phys. Lett.* **228**, 284 (1994).

¹⁰K. S. Smirnov, *Chem. Phys. Lett.* **229**, 250 (1994).

¹¹S. Fritzsche, M. Wolfsberg, R. Haberlandt, P. Demontis, G. B. Suffritti, and A. Tilocca, *Chem. Phys. Lett.* **296**, 253 (1998).

¹²R. Chitra and S. Yashonath, *Chem. Phys. Lett.* **234**, 16 (1995).

¹³K. Hahn, J. Kärger, and V. Kukla, *Phys. Rev. Lett.* **76**, 2762 (1995).

¹⁴P. Demontis, G. B. Suffritti, and A. Tilocca, *J. Chem. Phys.* **105**, 5586 (1996).

¹⁵S. Fritzsche, R. Haberlandt, G. Hofmann, J. Kärger, K. Heinzinger, and M. Wolfsberg, *Chem. Phys. Lett.* **265**, 253 (1997).

¹⁶V. Gupta, S. S. Nivarthi, A. V. McCormick, and H. T. Davis, *Chem. Phys. Lett.* **247**, 596 (1995).

¹⁷H. Jobic, K. Hahn, J. Kärger, M. Bee, A. Tuel, M. Noack, I. Girnus, and G. J. Kearley, *J. Phys. Chem. B* **101**, 5834 (1997).

¹⁸D. Keffer, A. V. McCormick, and H. T. Davis, *Mol. Phys.* **87**, 367 (1996).

¹⁹W. O. Haag and N. Y. Chen, in *Catalyst Design, Progress and Perspectives*, edited by L. L. Hegedus (Wiley-Interscience, New York, 1987).

²⁰J. Kärger, M. Petzold, H. Pfeifer, S. Ernst, and J. Weitkamp, *J. Catal.* **136**, 283 (1992).

²¹D. Keffer, Ph.D. dissertation, University of Minnesota, March 1996.

²²M. P. Allen and D. J. Tildesley, *Computer Simulations of Liquids* (Clarendon, Oxford, 1987).

²³J. M. Bennett, J. P. Cohen, E. M. Flanigen, J. J. Pluth, and J. V. Smith, *ACS Symp. Ser.* **218**, 109 (1983).

²⁴G. J. Kramer, N. P. Farragher, B. W. H. van Beest, and R. A. van Santen, *Phys. Rev. B* **43**, 5068 (1991).

²⁵A. J. M. de Man, W. P. J. H. Jacobs, J. P. Gilson, and R. A. van Santen, *Zeolites* **12**, 826 (1992).

²⁶S. Murad, D. J. Evans, and K. E. Gubbins, *Mol. Phys.* **37**, 725 (1979).

²⁷A. K. Rappe, C. J. Casewit, K. S. Colwell, W. A. Goddard III, and W. M. Skiff, *J. Am. Chem. Soc.* **114**, 10024 (1992).

²⁸S. D. Stoddard and J. Ford, *Phys. Rev. A* **8**, 1504 (1973).

²⁹W. B. Streett, D. J. Tildesley, and G. Saville, in *Computer Modelling of Matter: ACS Symposium Series Vol. 86*, edited by P. Lykos (American Chemical Society, Washington, 1978), p. 144.

³⁰J. J. Nicolas, K. E. Gubbins, W. B. Streett, and D. J. Tildesley, *Mol. Phys.* **37**, 1429 (1979).

³¹J. G. Powles, W. A. B. Evans, and N. Quirke, *Mol. Phys.* **46**, 1347 (1982).

³²D. J. Evans and S. Murad, *Mol. Phys.* **34**, 327 (1977).

³³R. L. June, A. T. Bell, and D. N. Theodorou, *J. Phys. Chem.* **94**, 8232 (1990).

³⁴A. V. Kiselev, A. A. Lopatkin, and A. A. Shulga, *Zeolites* **5**, 261 (1985).

³⁵R. J.-M. Pellenq and D. Nicholson, *J. Phys. Chem.* **98**, 13339 (1994).

³⁶R. J.-M. Pellenq and D. Nicholson, *Langmuir* **11**, 1626 (1995).

³⁷V. Lachet, A. Boutin, R. J.-M. Pellenq, D. Nicholson, and A. H. Fuchs, *J. Phys. Chem.* **100**, 9006 (1996).